Journal of Materials Chemistry C

PAPER

View Article Online
View Journal | View Issue

Cite this: J. Mater. Chem. C, 2014, 2, 7796

Novel near-infrared and multi-colored electrochromic polybenzoxazines with electroactive triarylamine moieties†

Lu-Chi Lin,‡[a] Hung-Ju Yen,‡[a] Yu-Ruei Kung,[b] Chyi-Ming Leu,[b] Tzong-Ming Lee[b] and Guey-Sheng Liou*[a]

Received 7th July 2014
Accepted 24th July 2014

DOI: 10.1039/c4tc01469c

www.rsc.org/MaterialsC

Two triarylamine-containing flexible polybenzoxazine films with T_g up to 312 °C were prepared by the thermally induced curing reaction of the corresponding polybenzoxazine precursors, which were synthesized by the reaction of paraformaldehyde with bisphenol A and 4,4′-diamino-4″-methoxytriphenylamine (**1**) or *N*,*N*′-bis(4-aminophenyl)-*N*,*N*′-di(4-methoxyphenyl)-1,4-phenylenediamine (**2**). By introduction of triarylamine units into the polybenzoxazine precursors, the resulting solution-processable polybenzoxazine precursor films not only exhibited interesting multi-colored electrochromic behavior with a high contrast ratio both in the visible range and near infrared region (NIR) but also could effectively increase the oxidation stages when compared with their corresponding polyamides.

Introduction

Electrochromism can be defined as the reversible change in optical properties of a material resulting from electrochemically induced redox states when adequate electrical current or potential is applied. The new or different visible region bands could be generated in the switching of reduction or oxidation.[1] Color changes are common between a transparent state, the chromophore only absorbs in the UV region, and a colored state, or between two colored states in a given electrolyte solution. Electrochromic (EC) anti-glare car rear-view mirrors have already been commercialized, and other proposed applications of EC materials including controllable light-reflective or light-transmissive devices in the visible region (*e.g.*, 400–800 nm) and near infrared region (NIR; *e.g.*, 800–2000 nm) for optical switching devices, data storage, sunglasses, controllable aircraft canopies for the military, and smart windows for cars and buildings also attracted great attention in recent years.[2] In addition, a wide variety of EC materials have been developed until now, which can be classified into five distinct families including metal oxides such as tungsten trioxide (WO_3) or iridium dioxide (IrO_2),[3] coordination complexes such as Prussian blue and phthalocyanines,[4] small organic molecules such as viologens,[5] conjugated polymers,[6–9] and arylamine-based polymers which are generally colorless unless undergoing charge-transfer interaction with an electron-deficient acceptor species.[10] Since 2005, our group has focused on anodically coloring high-performance polymers (*e.g.*, aromatic polyamides and polyimides) utilizing the triphenylamine (TPA) units as hole-transporting and EC functional moieties,[10a] which switch from the highly transmissive neutral state to oxidized color states with good electrochromic reversibility in the visible region or NIR range and could be differentiated on the basis of the method of increasing coloring stages.[10k] We also demonstrated that the incorporation of electron-donating substituents at the *para*-position of phenyl groups on the electrochemically active sites of the TPA units could effectively reduce the oxidation potential associated with enhancing electrochemical and EC stability.[10b,h,i] Moreover, the incorporation of packing-disruptive TPA units into the polymer backbone will result in good organo-solubility of the obtained polymers; thus, transparent and flexible polymer thin films can be easily prepared by solution casting and spin-coating techniques. This is beneficial for the fabrication of large-scale thin-film EC devices.

Polybenzoxazine (PB) is a well-known phenolic system with a wide range of interesting features and the capability to overcome several shortcomings of conventional novolac and resole type phenolic resins. These materials exhibit the following advantages: (a) near-zero volumetric change upon curing, (b) low water absorption, (c) excellent heat resistance, (d) no need of catalysts for curing and no release of toxic by-products during curing, (e) good mechanical properties and dimension stability, and (f) low dielectric constant.[11,12] Thus, PBs are widely used in the areas of electrical insulation, electrical encapsulation, and

[a]*Functional Polymeric Materials Laboratory, Institute of Polymer Science and Engineering, National Taiwan University, 1 Roosevelt Rd, 4th Sec., Taipei 10617, Taiwan. E-mail: gsliou@ntu.edu.tw*

[b]*Material and Chemical Research Laboratories, Industrial Technology Research Institute, 195, 4th Sec., Chung Hsing Rd., Hsinchu, Taiwan*

† Electronic supplementary information (ESI) available: Table: inherent viscosity, molecular weight and solubility behavior. Figure: ^{13}C NMR spectra of PB precursors, **TPA-BPA** and **TPPA-BPA**; electrochromic behavior of **P(TPA-BPA)**. See DOI: 10.1039/c4tc01469c

‡ These authors contributed equally to this work.

aeronautical and astronautical technologies. PBs can be prepared by the thermal curing reaction of monofunctional[13] or bifunctional benzoxazines,[11b,14] while these kinds of PBs can only exist in the bulk type because of low molecular weights. In order to obtain the film type PBs, a new concept for the development of benzoxazines was first proposed by Takeichi in 2005 by the curing reaction of PB precursors with higher molecular weights.[15] Then, Ishida[16] and Yagci[17] have also prepared a series of oligobenzoxazines. However, these approaches suffer from branching and side reactions; therefore, the resultant molecular weight of PBs prepared by Mannich-type polycondensation was limited until the solvent effect on the polycondensation was examined by Lin in 2012.[18] They found that PB precursors prepared in toluene–ethanol exhibit higher purity and molecular weight than those prepared in chloroform used by Takeichi's group. Therefore, the cured PB films with good flexibility and thermal properties can be obtained by this approach.

In this study, two TPA-based diamines, 4,4′-diamino-4″-methoxytriphenylamine (**1**)[10b] and *N*,*N*′-bis(4-aminophenyl)-*N*,*N*′-di(4-methoxyphenyl)-1,4-phenylenediamine (**2**),[10h] were used to synthesize novel high molecular weight TPA-containing PB precursors with good film-forming capability. Then, the corresponding flexible PB films with excellent thermal stability could be readily obtained by the curing reaction of the PB precursors. Thus, these TPA-containing PBs are successfully prepared and reported for the first time to date to the best of our knowledge, and we anticipated that the resulting novel EC PB precursors and PBs would have excellent EC behavior with high optical transmittance change (Δ%*T*) both in visible and NIR regions.

Results and discussion

Synthesis of polybenzoxazine precursors

Two novel PB precursors were synthesized by Mannich-type polycondensation of paraformaldehyde, bisphenol A, and diamines, 4,4′-diamino-4″-methoxytriphenylamine (**1**)[10b] and *N*,*N*′-bis-(4-aminophenyl)-*N*,*N*′-di(4-methoxyphenyl)-1,4-phenylenediamine (**2**),[10h] using toluene–ethanol as a co-solvent (Scheme 1) according to the previous literature.[18a]

All Mannich-type polycondensation reactions proceeded homogeneously and PB precursors with high molecular weights could be obtained (Table S1†). The structures of the PB precursors were confirmed by ^{1}H NMR and ^{13}C NMR spectroscopy, and a typical set of ^{1}H and ^{13}C NMR spectra of the novel PB precursors are shown in Fig. 1 and S1,† respectively. The characteristic oxazine peaks at 5.2 ppm and 4.5 ppm in ^{1}H spectra confirm the structure of benzoxazines. Furthermore, the

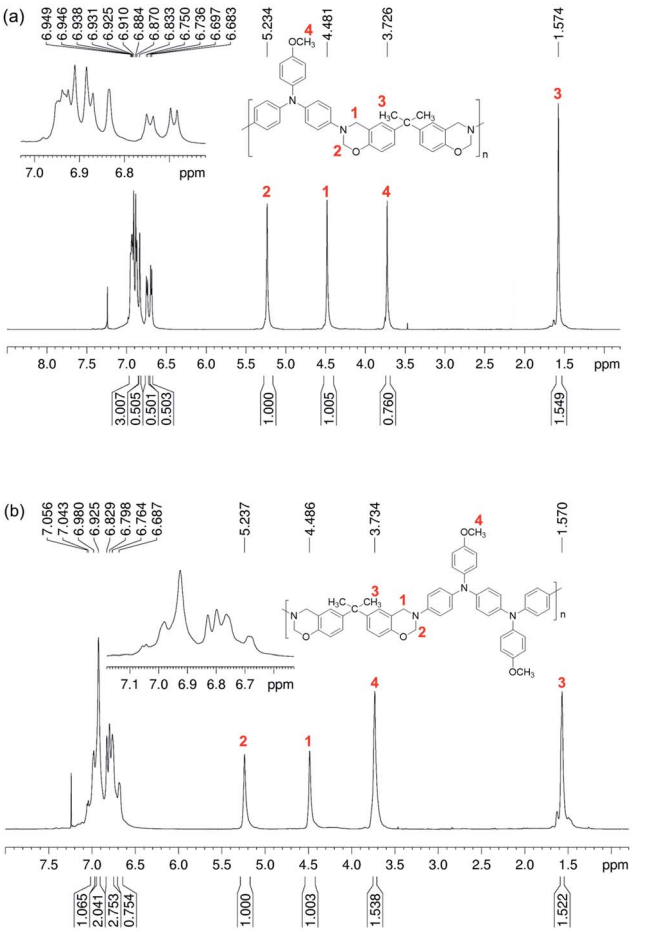

Fig. 1 ^{1}H NMR spectra of (a) TPA-BPA and (b) TPPA-BPA in $CDCl_3$.

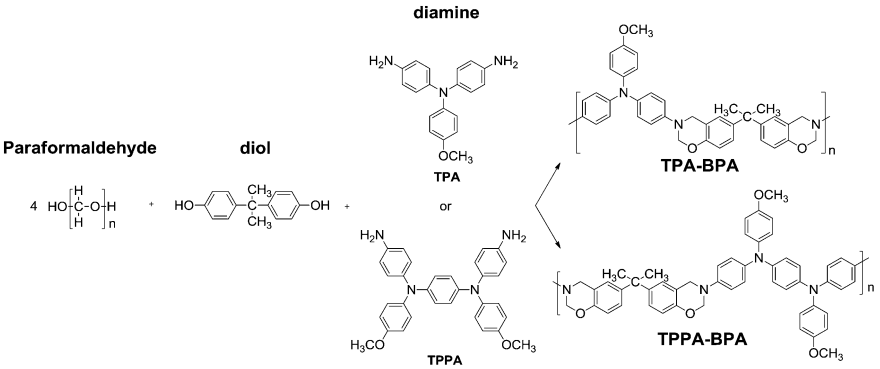

Scheme 1 Synthesis of the polybenzoxazine precursors.

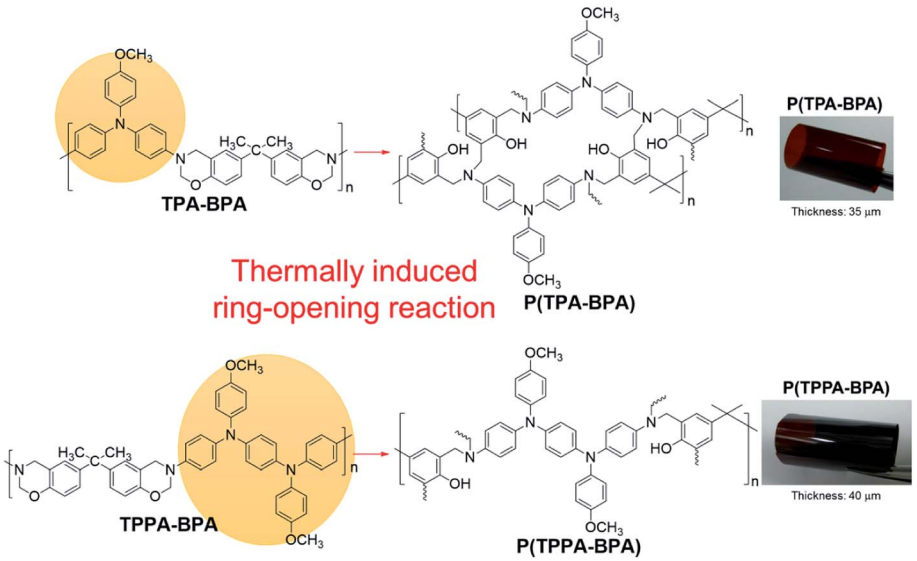

Scheme 2 Thermally induced ring-opening reactions of the polybenzoxazine precursors to the corresponding polybenzoxazines, P(TPA-BPA) and P(TPPA-BPA). The photographs show the appearance of these polybenzoxazine films.

tough and cross-linked PB films could be successfully prepared by the thermally induced ring-opening reaction from the high-molecular weight PB precursors (Scheme 2).

Basic characterization

Solubility behavior of the PB precursors was investigated qualitatively, and the results are summarized in Table S2.† The resulting PB precursors showed good solubility in many organic solvents due to packing-disruptive triarylamine moieties in the polymer backbone, making these PB precursors potential candidates for practical applications by spin-coating or inkjet-printing processes to afford high performance thin films for optoelectronic devices.

As shown in Fig. 2(a), the thermally induced ring-opening reaction was identified by the DSC measurement, and the exothermic peak temperatures of **TPA-BPA** and **TPPA-BPA** were recorded to be 270 °C and 262 °C, respectively. The thermal properties of the cured PB films were investigated by TGA, TMA, and DMA, and the results are summarized in Table 1. Typical TGA curves of TPA-based PBs are depicted in Fig. 2(b). These cured TPA-containing PBs showed good thermal stability with insignificant weight loss up to 350 °C both in nitrogen and air atmospheres. The amount of carbonized residues (char yield)

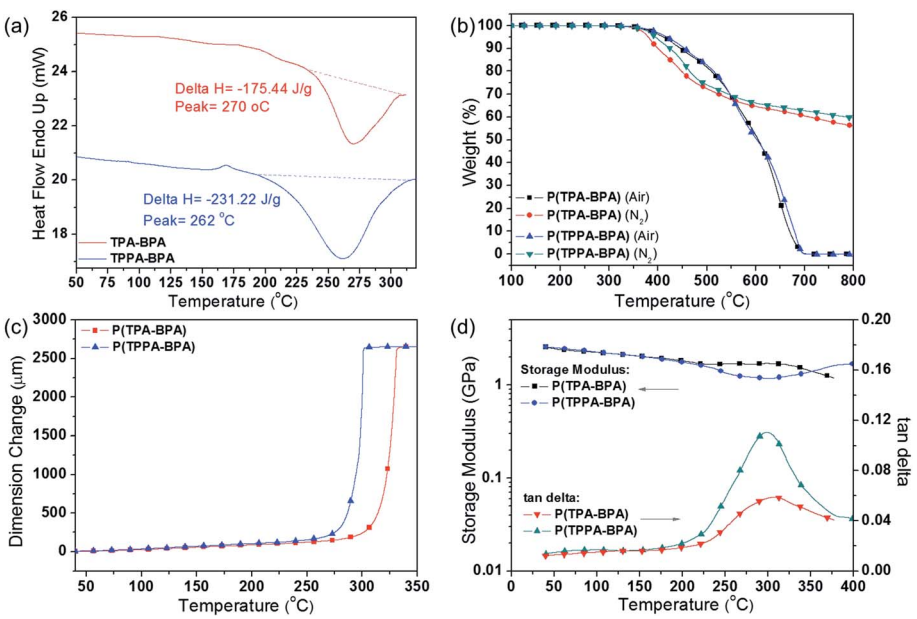

Fig. 2 (a) DSC thermograms of polybenzoxazine precursors; (b) TGA, (c) TMA, and (d) DMA thermograms of the cured polybenzoxazine films.

Table 1 Thermal properties of polybenzoxazines, P(TPA-BPA) and P(TPPA-BPA)

Polymer	T_g[a] (°C)	CTE[b] (ppm °C^{-1})	T_g[c] (°C)	T_d^{5d} (°C) Air	T_d^{5d} (°C) N_2	T_d^{10d} (°C) Air	T_d^{10d} (°C) N_2	R_{w800}[e] (%)	LOI[f]
P(TPA-BPA)	312	56	311	410	380	445	400	56	40
P(TPPA-BPA)	288	65	298	420	395	455	425	60	42

[a] Glass transition temperature measured by TMA using the film/fiber mode with a constant applied load of 50 mN at a heating rate of 10 °C min^{-1}. [b] Coefficient of linear thermal expansion between 50 °C and 200 °C measured by TMA using the film/fiber mode with a constant applied load of 50 mN at a heating rate of 10 °C min^{-1}. [c] Glass transition temperature measured by DMA using the film/fiber at a heating rate of 3 °C min^{-1}. [d] Temperature at which 5% and 10% weight loss occurred, respectively, recorded by TGA at a heating rate of 20 °C min^{-1} and a gas flow rate of 20 cm^3 min^{-1}. [e] Residual weight percentages at 800 °C under nitrogen flow. [f] LOI = Limiting Oxygen Index = (17.5 + 0.4 × char yield) at 800 °C.

measured in a nitrogen atmosphere at 800 °C and calculated limiting oxygen index (LOI) values of these PBs are higher than 56% and 40, respectively, which could be ascribed to their high aromatic unit content. In addition to good thermal stability, these thermoset PBs also possessed high glass-transition temperatures (T_g) of 312 and 284 °C measured by TMA (Fig. 2(c)). Furthermore, the T_g values taken from the tan δ peak in DMA thermograms (Fig. 2(d)) were 311 and 298 °C for **TPA-BPA** and **TPPA-BPA**, respectively, and the results are similar to that of TMA data. The results showed that the novel triarylamine-based PBs have remarkable thermal properties as opposed to the PBs without TPA units.

Table 2 Electrochemical properties of all the resulting polymers

	Oxidation potential[a] (V) E_{onset}	$E_{1/2(ox1)}$	$E_{1/2(ox2)}$	$E_{1/2(ox3)}$	$E_{p(ox4)}$
TPA-BPA	0.40	0.51	0.81	1.12	—
P(TPA-BPA)	0.71	0.95	—	—	—
TPPA-BPA	0.43	0.59	0.81	1.02	1.41
P(TPPA-BPA)	0.45	0.66	0.97	—	—

[a] From cyclic voltammograms *vs.* Ag/AgCl in CH_3CN. $E_{1/2}$: average potential of the redox couple peaks. E_p: peak potential of the irreversible fourth oxidation step.

Electrochemical properties

The electrochemical properties of the PB precursors and PBs in the film state were investigated by cyclic voltammetry (CV) in anhydrous acetonitrile (CH_3CN), using 0.1 M tetrabutylammonium perchlorate (TBAP) as a supporting electrolyte under a nitrogen atmosphere, and the results are depicted and summarized in Fig. 3 and Table 2, respectively. PB precursors, **TPA-BPA** and **TPPA-BPA**, both reveal three reversible oxidation couples with E_{onset} at 0.40 V and 0.43 V, respectively (Fig. 3(a) and (b)). Meanwhile, **TPPA-BPA** showed an additional E_p at 1.41 V. Furthermore, the electrochemical properties of the corresponding cured PBs, **P(TPA-BPA)** and **P(TPPA-BPA)**, were also investigated (Fig. 4). Before electrochemical measurement, prescanning was utilized to make the thermoset PB thin films become a saturated state. However, only one reversible oxidation redox stage (E_{onset} = 0.71) for **P(TPA-BPA)** and two reversible oxidation redox stages (E_{onset} = 0.45 V) for **P(TPPA-BPA)**, respectively, could be observed. The decreased oxidation stages of cross-linked PBs as oppose to that of PB precursors may ascribe to the formation of intramolecular hydrogen bonding between the active nitrogen sites of TPA-based diamine moieties and hydroxyl groups of the bisphenol A units in the network structures of PBs as shown in Scheme 3, which resulted in lowering of the electron-donating ability of the electro-active nitrogen sites of the triarylamine diamine moieties in the cured PBs. **P(TPPA-BPA)** films exhibited moderate electrochemical stability at both first and second oxidation stages after 100 continuous cyclic scans (Fig. 4). During the electrochemical oxidation of the thin film of PBs or PB precursors, the color of the polymer film changed from colorless to green, blue, and blackish blue. The purposed oxidation states corresponding to the color changes are also summarized in Scheme 3.

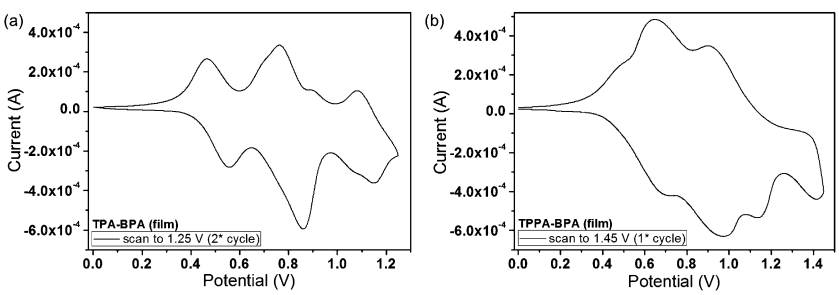

Fig. 3 (a) CV diagrams of the TPA-BPA film and (b) the TPPA-BPA film in 0.1 M TBAP/CH_3CN at a scan rate of 50 mV s^{-1}.

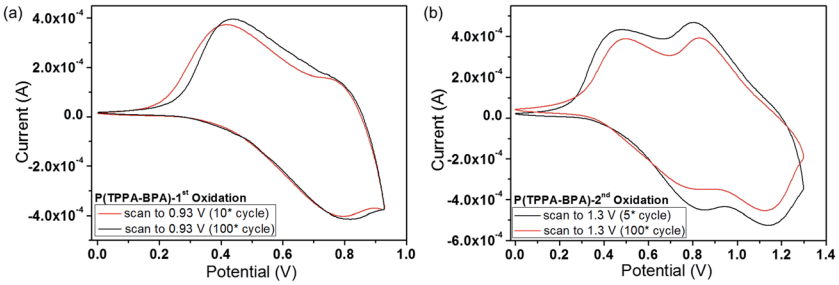

Fig. 4 (a) First oxidation and (b) second oxidation cyclic voltammetric diagrams of the P(TPPA-BPA) film in 0.1 M TBAP/CH_3CN at a scan rate of 50 mV s^{-1}.

Spectroelectrochemistry properties

The optical behavior of the EC films was evaluated by spectroelectrochemical experiments. For the investigations, the thin films of PB precursors and PBs were cast on an ITO-coated glass slide, and a homemade electrochemical cell was built from a commercial cuvette. The sample cell was placed in the optical path of the light beam in a UV-vis-NIR spectrophotometer to acquire optical absorption spectra under various applied potentials in TBAP–CH_3CN solution. Fig. 5 shows a series of optical absorbance curves of the resulting PB precursors with correlated applied potentials. The **TPA-BPA** colorless film exhibited strong characteristic absorption at 310 nm, characteristic for the π–π* transition of the TPA moieties in the neutral form (0 V) as shown in Fig. 5(a). Upon oxidation (increasing the applied voltage from 0 to 0.62 V), the intensity of the absorption peak at 310 nm gradually decreased, whereas the intensity of new peaks at 386 nm and 688 nm increased. Besides, a broad band with maximum absorption at 930 nm in the near infrared (NIR) region gradually increased in intensity. The spectral change in visible-light region could be attributed to the formation of a stable monocation radical of the TPA moiety corresponding to **TPA-BPA**$^{+\cdot}$. In addition, the broad characteristic absorption band in the NIR region could be ascribed to the strong electronic coupling (the electron is delocalized over the two redox centers through a phenyl bridge), leading to intervalence charge transfer (IV-CT) excitation through the phenyl bridge between active neutral nitrogen atom and cation radical nitrogen of the TPA moiety, which was consistent with the phenomenon classified by Robin and Day.[19] As the anodic potential increases to 0.89 V corresponding to **TPA-BPA**$^{2+}$, the absorption bands of the cation radical decreased gradually with a new broad band centered at around 811 nm. The disappearance of the NIR absorption band can be attributed to the formation of *p*-phenylenediamine quinonoid-type dication after second oxidation occurred at the dialkyl-substituted amino groups thus eliminating the IV-CT. Unfortunately, the film of the PB precursor, **TPA-BPA**, dissolved gradually in solution upon oxidation, and hence we could not investigate the absorption spectra change at the third oxidation stage.

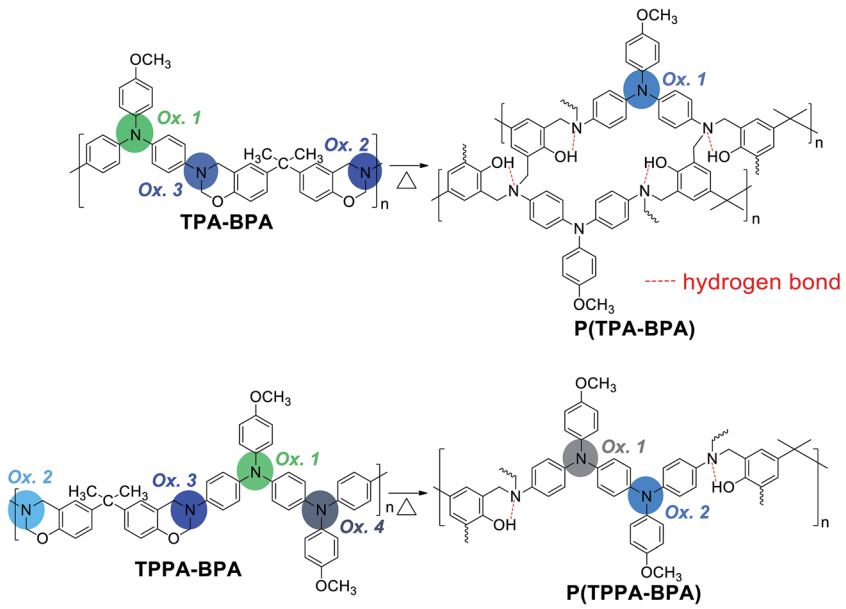

Scheme 3 Intramolecular hydrogen bonding in the network structures of polybenzoxazines as well as the color change of the polymer film corresponding to each oxidation step.

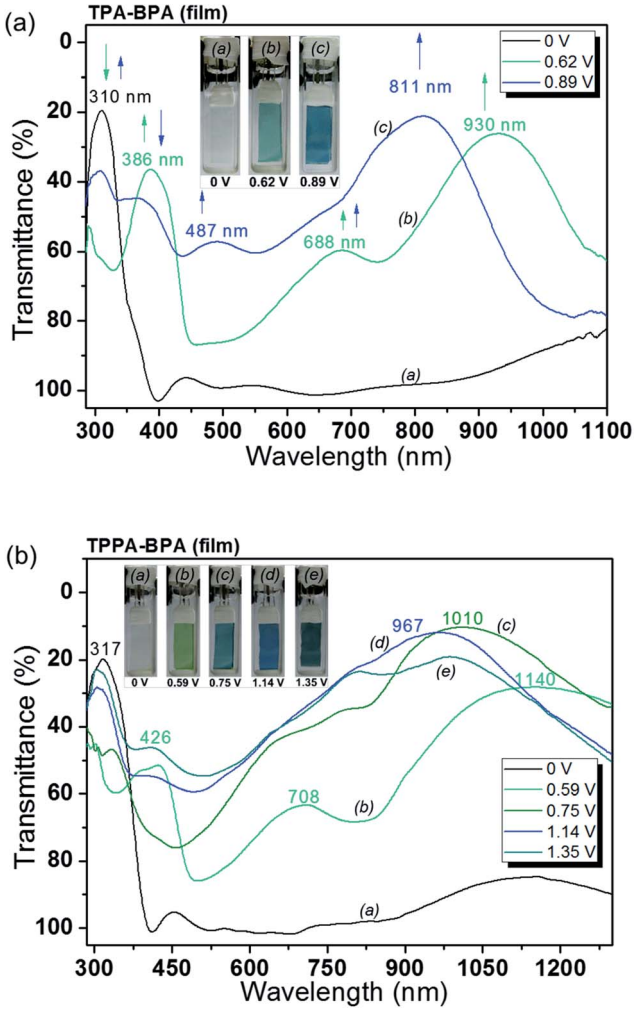

Fig. 5 Electrochromic behavior of (a) the **TPA-BPA** thin film (110 nm) and (b) the **TPPA-BPA** thin film (125 nm) in 0.1 M TBAP/CH_3CN.

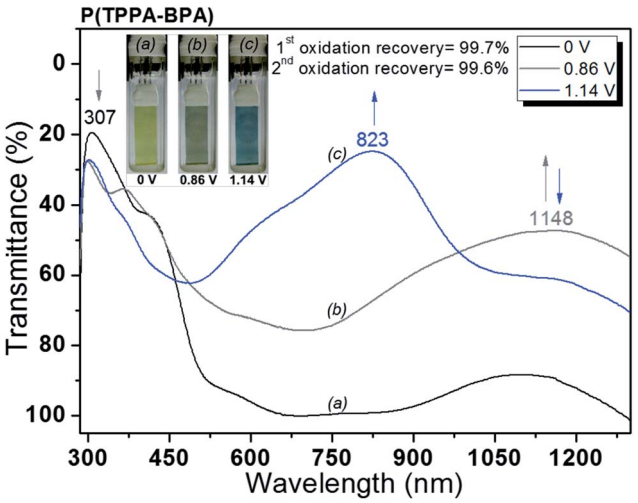

Fig. 6 Electrochromic behavior of the **P(TPPA-BPA)** film (125 nm) in 0.1 M TBAP/CH_3CN.

For PB precursor **TPPA-BPA** shown in Fig. 5(b), the colorless **TPPA-BPA** film also exhibited strong characteristic absorption at 317 nm of TPA in the neutral form (0 V). As the applied potential increased from 0 to 0.59 V, the intensity of the absorption peak at 317 nm decreased, while new peaks at 426 and 1140 nm gradually increased in intensity. The characteristic broad absorption around 1140 nm in the NIR region resulted from the IV-CT excitation of the **TPPA-BPA** cation radical similar to that of the **TPA-BPA** film. As the anodic potential increased to 0.75 V, the nitrogen atom of dialkyl-substituted amino groups was oxidized resulting in enhanced IV-CT broad absorption around 1010 nm in the NIR region. Further increasing the applied potential to 1.14 V, the absorption bands of cation radical decreased gradually with a new broad band centered at around 967 nm. The disappearance of the NIR absorption band could be attributed to the further oxidation from monocation radical species to the formation of quinonoid-type dication in the other nitrogen atoms of dialkyl-substituted amino groups. When the oxidation potential was higher than 1.35 V, the NIR region absorbance decreased continuously as in the case of **TPA-BPA**$^{2+}$. It is worthy to mention that the introduction of TPA derivatives into PB precursors could effectively increase the oxidation stages and reveal multi-colored EC behaviors due to the increasing number of tertiary amines in the repeat units of the resulting PB precursors as applications in the epoxy system[10m,n] but as opposed to their corresponding polyamides.[10b,h] The color of PB precursor films changed distinctly from colorless to green, blue, and blackish blue during the electrochemical oxidation of the PB precursor thin films as shown in Fig. 5.

The EC properties of thermoset PBs, **P(TPPA-BPA)** and **P(TPA-BPA)** prepared by the thermally induced ring-opening reactions of the corresponding PB precursors, were also investigated and are shown in Fig. 6 and S2,† respectively. In the neutral form (0 V), these yellowish films exhibited strong TPA characteristic absorption at around 305 nm. Upon oxidation of **P(TPA-BPA)** (increasing the applied voltage from 0 to 1.08 V), the intensity of the absorption peaks at 300 nm and 404 nm gradually decreased, whereas two new peaks grew up at 493 nm and 794 nm. The new spectral patterns were assigned as those of the cationic radicals, formed by electron removal from the lone pair of the nitrogen atom on the TPA units causing the structure to flatten off and delocalize, resulting in bathochromic absorption of the TPA cation radicals at longer wavelengths. On the other hand, the results of **P(TPPA-BPA)** films are illustrated in Fig. 6 during oxidation (increasing the applied voltage from 0 to 0.86 V). The intensity of the absorption peak at 307 nm gradually decreased, while a new peak at 1148 nm gradually increased in intensity. The broad absorption wavelength around 1148 nm in the NIR region resulted from the IV-CT excitation of **P(TPPA-BPA)** similar to the behavior of the first oxidation stage of the **TPA-BPA** film. When the applied potential was further increased to 1.14 V, the IV-CT absorption bands of the cation radical in the NIR region decreased gradually with the increase of a new broad band centered at around 823 nm. The disappearance of the NIR absorption band could be attributed to the further oxidation from monocation radical species to the formation of quinonoid-

type dication in the other nitrogen atoms of *p*-phenylenediamine quinonoid-type dication as in the case of the second oxidation stage of the corresponding polyamides.[10h] In addition, **P(TPPA-BPA)** films also revealed excellent EC stability at both first and second oxidation stages with the reversibility of up to 99.7 and 99.6%, respectively (Fig. 6) as the results of structure-related polyamides published previously.[10g,i]

For EC switching studies, polymer films were cast on ITO-coated glass slides in the same manner as described above, and chronoamperometric and absorbance measurements were performed. While the films were switched, the absorbance at given wavelength was monitored as a function of time using UV-vis-NIR spectroscopy. Switching data for the representative cast film of **P(TPPA-BPA)** are shown in Fig. S3,† exhibiting moderate EC stability and a high contrast ratio for both first and second oxidation states.

Conclusions

Two novel anodically TPA-containing EC PBs were successfully prepared by the thermal curing reaction of the corresponding PB precursors, which were synthesized by the reaction of paraformaldehyde with bisphenol A and TPA-based diamines. The resulting TPA-based PBs exhibited good thermal properties and interesting multi-colored behavior with highly optical contrast both in visible and NIR regions. To the best of our knowledge, this is the first time the EC behaviors of PB precursors and PBs with TPA moieties have been explored and investigated. Compared with their corresponding polyamides, these two TPA-based PB precursors not only reveal lower oxidative potentials but also increased the oxidation stages due to the introduction of the TPA-based diamines. Thus, these resulting polymers have potential to be the candidates for anodically EC applications due to their interesting multi-colored EC behavior.

Experimental section

Materials

4,4′-Diamino-4″-methoxytriphenylamine[10b] (**1**, mp = 148–149 °C) and *N*,*N*′-bis(4-aminophenyl)-*N*,*N*′-di(4-methoxyphenyl)-1,4-phenylenediamine[10h] (**2**, mp = 206–209 °C) were synthesized according to the previously reported procedures.

Synthesis of polybenzoxazine precursors

The synthesis of **TPA-BPA** was used as an example to illustrate the general synthetic route for the resulting PB precursor. 1.0 g (3.27 mmol) of **1**, 0.75 g (3.27 mmol) of bisphenol A, and 7.2 mL mixed solvent of toluene–ethanol (2/1, v/v) were introduced into a round-bottom 50 mL glass flask equipped with a nitrogen inlet, a condenser, and a magnetic stirrer. Paraformaldehyde 0.39 g (13.08 mmol) was added to the reaction mixture after increasing the temperature to 70 °C. Then, the mixture was stirred at 85 °C for 2 days. The solution was then poured into methanol, and the obtained precipitate was filtered and washed in methanol at a reflux temperature. After drying at 80 °C in a vacuum oven, yellow powder (1.80 g, 95% yield) was obtained. ^{1}H NMR ($CDCl_3$, δ, ppm): 1.57 (s, 6H, CH_3), 3.73 (s, 3H, OCH_3), 4.48 (s, 4H, N–CH_2-Ar), 5.23 (s, 4H, N–CH_2–O), 6.69 (d, 2H), 6.74 (d, 2H), 6.83 (s, 2H), 6.95 (m, 12H). ^{13}C NMR ($CDCl_3$, δ, ppm): 31.0, 41.7, 50.8, 55.4, 79.8, 114.5, 116.3, 119.4, 120.1, 123.9, 124.6, 125.8, 126.3, 141.3, 142.5, 143.1, 143.2, 152.2, 155.3.

Preparation of polybenzoxazine thick films

The preparation of **P(TPA-BPA)** was used as an example to illustrate the general route used to produce the thermoset PB thick films. A 25 wt% PB precursor in *N*-methyl-2-pyrrolidone (NMP) solution was prepared. The solution was then cast onto glass and dried at 100 °C for 3 h, and then cured at 120 °C (2 h), 160 °C (1 h), 200 °C (1 h), 240 °C (1 h), and 260 °C (1 h) in vacuum. The thickness of the obtained PB films was about 40 ± 5 μm and was used for the study of thermal properties.

Preparation of polybenzoxazine precursor thin films

The preparation of **TPA-BPA** was used as an example to illustrate the general route used to produce the thin films of PB precursors. A solution was prepared by dissolving the PB precursor, **TPA-BPA**, in 1,4-dioxane at a concentration around 30 mg mL^{-1}. The solution was filtered through a 0.2 μm syringe filter and was spin-coated at 1500 rpm for 20 seconds onto an indium tin oxide (ITO) glass substrate. The obtained thin films with a thickness of 120 ± 10 nm were used for electrochemical and spectroelectrochemical tests.

Preparation of polybenzoxazine thin films

The preparation of **P(TPA-BPA)** was used as an example to illustrate the general route used to produce the thermoset PB thin films. The PB thin film, **P(TPA-BPA)**, was prepared by curing the thin film of PB precursor **TPA-BPA** at a heating program of 100 °C, 140 °C, 180 °C, 220 °C, and 260 °C each for 1 h, respectively, in vacuum. The obtained thin films with a thickness of 120 ± 10 nm were used for electrochemical and spectroelectrochemical tests.

Measurements

^{1}H NMR and ^{13}C NMR spectra were recorded on a Bruker AVANCE-600 FT-NMR using tetramethylsilane as the internal standard, and peak multiplicity was reported as follows: s, singlet; d, doublet. The inherent viscosities were determined at 0.5 g dL^{-1} concentration using a Tamson TV-2000 viscometer at 30 °C. Gel permeation chromatographic (GPC) analysis was carried out on a Waters chromatography unit interfaced with a Waters 2410 refractive index detector. Two Waters 5 μm Styragel HR-2 and HR-4 columns (7.8 mm I. D. × 300 mm) were connected in series with NMP as the eluent at a flow rate of 0.5 mL min^{-1} at 40 °C and were calibrated with polystyrene standards. For temperature scanning, DSC analyses were performed on a PerkinElmer Pyris 1 DSC at a scan rate of 10 °C min^{-1} in flowing nitrogen (20 cm^3 min^{-1}). Thermogravimetric analyses (TGA) were conducted with a PerkinElmer Pyris 1 TGA. Experiments were carried out on approximately 3–5 mg film samples heated in flowing nitrogen or air (flow rate = 20 cm^3 min^{-1}) at a heating

rate of 20 °C min^{-1}. Thermal Mechanical Analysis (TMA) was conducted with a TA instrument TMA Q400. The TMA experiments were conducted at a scan rate of 10 °C min^{-1} with a film/fiber probe under an applied constant load of 50 mN. Dynamic mechanical thermal analysis (DMTA) was performed using a DMA 2980, TA Instruments (USA), at a heating rate of 3 °C min^{-1} with a load frequency of 1 Hz in tension mode in air. Electrochemistry was performed with a CH Instruments 612C electrochemical analyzer. Voltammograms were presented with the positive potential pointing to the right and with increasing anodic currents pointing downwards. Cyclic voltammetry (CV) was conducted with the use of a three-electrode cell in which the cast film on an ITO (the area of the resulting polymer thin films was about 2.0 cm × 0.8 cm) coated glass slide acts as the working electrode in anhydrous acetonitrile (CH_3CN). A platinum wire was used as an auxiliary electrode. All cell potentials were taken by using a homemade Ag/AgCl, KCl (sat.) reference electrode. Spectroelectrochemical experiments were carried out in a cell built from a 1 cm commercial UV-vis cuvette using a Hewlett-Packard 8453 UV-vis diode array and a Hitachi U-4100 UV-vis-NIR spectrophotometer. The ITO-coated glass slide or glassy carbon was used as the working electrode, a platinum wire as the counter electrode, and an Ag/AgCl cell as the reference electrode. The thickness of the resulting polymer thin films was measured using an alpha-step profilometer (Kosaka Lab., Surfcorder ET3000, Japan).

Acknowledgements

The authors gratefully acknowledge the National Science Council of Taiwan for the financial support.

Notes and references

1 P. M. S. Monk, R. J. Mortimer and D. R. Rosseinsky, *Electrochromism: Fundamentals and Applications*, VCH, Weinheim, Germany, 1995.

2 (*a*) M. Green, *Chem. Ind.*, 1996, **17**, 641; (*b*) R. J. Mortimer, *Chem. Soc. Rev.*, 1997, **26**, 147; (*c*) T. L. Rose, S. D'Antonio, M. H. Jillson, A. B. Kon, R. Suresh and F. Wang, *Synth. Met.*, 1997, **85**, 1439; (*d*) P. Topart and P. Hourquebie, *Thin Solid Films*, 1999, **352**, 243; (*e*) E. B. Franke, C. L. Trimble, J. S. Hale, M. Schubert and J. A. Woollam, *J. Appl. Phys.*, 2000, **88**, 5777; (*f*) U. Bach, D. Corr, D. Lupo, F. Pichot and M. Ryan, *Adv. Mater.*, 2002, **14**, 845; (*g*) P. Chandrasekhar, B. J. Zay, T. McQueeney, A. Scara, D. Ross, G. C. Birur, S. Haapanen, L. Kauder, T. Swanson and D. Douglas, *Synth. Met.*, 2003, **23**, 135; (*h*) C. Ma, M. Taya and C. Xu, *Polym. Eng. Sci.*, 2008, **48**, 2224; (*i*) S. Beaupre, A. C. Breton, J. Dumas and M. Leclerc, *Chem. Mater.*, 2009, **21**, 1504.

3 W. C. Dautremont-Smith, *Displays*, 1982, **3**, 3.

4 N. R. de Tacconi, K. Rajeshwar and R. O. Lezna, *Chem. Mater.*, 2003, **15**, 3046.

5 C. J. Schoot, J. J. Ponjeé, H. T. van Dam, R. A. van Doorn and P. T. Bolwijn, *Appl. Phys. Lett.*, 1973, **23**, 64.

6 K. Bange and T. Bambke, *Adv. Mater.*, 1990, **2**, 10.

7 R. J. Mortimer, *Electrochim. Acta*, 1999, **44**, 2971.

8 R. J. Mortimer, A. L. Dyer and J. R. Reynolds, *Displays*, 2006, **27**, 2.

9 P. M. S. Monk, R. J. Mortimer and D. R. Rosseinsky, *Electrochromism and Electrochromic Devices*, Cambridge University Press, Cambridge, UK, 2007.

10 (*a*) S. H. Cheng, S. H. Hsiao, T. H. Su and G. S. Liou, *Macromolecules*, 2005, **38**, 307; (*b*) C. W. Chang, G. S. Liou and S. H. Hsiao, *J. Mater. Chem.*, 2007, **17**, 1007; (*c*) G. S. Liou and C. W. Chang, *Macromolecules*, 2008, **41**, 1667; (*d*) S. H. Hsiao, G. S. Liou, Y. C. Kung and H. J. Yen, *Macromolecules*, 2008, **41**, 2800; (*e*) C. W. Chang, C. H. Chung and G. S. Liou, *Macromolecules*, 2008, **41**, 8441; (*f*) C. W. Chang and G. S. Liou, *J. Mater. Chem.*, 2008, **18**, 5638; (*g*) G. S. Liou and H. Y. Lin, *Macromolecules*, 2009, **42**, 125; (*h*) H. J. Yen and G. S. Liou, *Chem. Mater.*, 2009, **21**, 4062; (*i*) H. J. Yen, H. Y. Lin and G. S. Liou, *Chem. Mater.*, 2011, **23**, 1874; (*j*) L. T. Huang, H. J. Yen and G. S. Liou, *Macromolecules*, 2011, **44**, 9595; (*k*) H. J. Yen and G. S. Liou, *Polym. Chem.*, 2012, **3**, 255; (*l*) H. J. Yen, C. J. Chen and G. S. Liou, *Adv. Funct. Mater.*, 2013, **23**, 5307; (*m*) Y. W. Chuang, H. J. Yen and G. S. Liou, *Chem. Commun.*, 2013, **49**, 9812; (*n*) Y. W. Chuang, H. J. Yen, J. H. Wu and G. S. Liou, *ACS Appl. Mater. Interfaces*, 2014, **6**, 3894.

11 (*a*) H. Ishida, in *Handbook of Benzoxazine Resins*, ed. H. Ishida and T. Agag, Elsevier, Amsterdam, 2011, pp. 3–81; (*b*) X. Ning and H. Ishida, *J. Polym. Sci., Part A: Polym. Chem.*, 1994, **32**, 1121.

12 (*a*) X. Ning and H. Ishida, *J. Polym. Sci., Part B: Polym. Phys.*, 1994, **32**, 921; (*b*) H. Ishida and D. Allen, *J. Polym. Sci., Part B: Polym. Phys.*, 1996, **34**, 1019; (*c*) Y. L. Hong and H. Ishida, *Macromolecules*, 1997, **30**, 1099; (*d*) Y. C. Su and F. C. Chang, *Polymer*, 2003, **44**, 7989; (*e*) N. N. Gosh, B. Kiskan and Y. Yagci, *Prog. Polym. Sci.*, 2007, **32**, 1344.

13 W. J. Burke, J. L. Bishop, E. L. M. Glennie and W. N. Bauer, *J. Org. Chem.*, 1965, **30**, 3423.

14 (*a*) N. Koichi, O. Masaaki and O. Kenji, Matsushita Electric Works, JP Kokai, 2005, vol. 21, p. 3301; (*b*) C. H. Lin, S. L. Chang, C. W. Hsieh and H. H. Lee, *Polymer*, 2008, **49**, 1220.

15 (*a*) T. Takeichi, T. Kano and T. Agag, *Polymer*, 2005, **46**, 12172; (*b*) T. Takeichi and T. Agag, *High Perform. Polym.*, 2006, **18**, 777.

16 (*a*) J. Liu, T. Agag and H. Ishida, *Polymer*, 2010, **51**, 5688; (*b*) M. Nakamura and H. Ishida, *Polymer*, 2009, **50**, 2688; (*c*) T. Agag, S. Geiger, S. M. Alhassan, S. Qutubuddin and H. Ishida, *Macromolecules*, 2010, **43**, 7122.

17 C. Altinkok, B. Kiskan and Y. Yagci, *J. Polym. Sci., Part A: Polym. Chem.*, 2011, **49**, 2445.

18 (*a*) C. H. Lin, S. L. Chang, T. Y. Shen, Y. S. Shih, H. T. Lin and C. F. Wang, *Polym. Chem.*, 2012, **3**, 935; (*b*) C. H. Lin, Y. S. Shih, M. W. Wang, C. Y. Tseng, T. Y. Juang and C. F. Wang, *RSC. Adv.*, 2014, **4**, 8692.

19 M. Robin and P. Day, *Adv. Inorg. Chem. Radiochem.*, 1967, **10**, 247.